Calibration of Low-Cost Particulate Matter Sensors PurpleAir: Model Development for Air Quality under High Relative Humidity Conditions

5 Martine E. Mathieu-Campbell[1], Chuqi Guo[2], Andrew P. Grieshop[3], Jennifer Richmond-Bryant[1,2]

[1] Center for Geospatial Analytics, North Carolina State University, Raleigh, NC 27695, USA
[2] Department of Forestry and Environmental Resources, North Carolina State University, Raleigh, NC 27695, USA
[3] Department of Civil, Construction and Environmental Engineering, North Carolina State University, Raleigh, NC 27695,
10 USA

Correspondence to: Jennifer Richmond-Bryant (jrbryan3@ncsu.edu)

15 **Abstract.** The primary source of measurement error from the widely-used particulate matter (PM) PurpleAir sensors is ambient relative humidity (RH). Recently, the U.S. EPA developed a national correction model for $PM_{2.5}$ concentrations measured by PurpleAir sensors (Barkjohn model). However, their study included few sites in the Southeastern U.S., the most humid region of the country. To provide high-quality spatial and temporal data and inform community exposure risks in this area, our study developed and evaluated PurpleAir correction models for use in the warm-humid climate zones of the U.S. We used hourly
20 PurpleAir data and hourly reference grade $PM_{2.5}$ data from the EPA Air Quality System database from January 2021 to August 2023. Compared with the Barkjohn model, we found improved performance metrics with error metrics decreasing by 16-23 % when applying a multi linear regression (MLR) model with RH and temperature as predictive variables. We also tested a novel semi-supervised clustering (SSC) method and found that a nonlinear effect between $PM_{2.5}$ and RH emerges around a RH of 50 % with slightly greater accuracy. Therefore, our results suggested that a clustering approach might be more accurate
25 in high humidity conditions to capture the non-linearity associated with PM particle hygroscopic growth.

1 Introduction

In recent years, many communities started using low-cost sensors for particulate matter with aerodynamic diameter smaller than 2.5 µm ($PM_{2.5}$) to predict community exposure risks (Bi et al., 2020, 2021; L. J. Chen et al., 2017; Jiao et al., 2016; Kim et al., 2019; Kramer et al., 2023; Lu et al., 2022; Snyder et al., 2013; Stavroulas et al., 2020), since short-term and long-term
30 exposures to $PM_{2.5}$ are associated with several adverse health effects (Brook et al., 2010; R. Chen et al., 2016; Cohen et al., 2017; Health Effects Institute, 2020; Landrigan et al., 2018; Olstrup et al., 2019; Pope & Dockery, 2006). These low-cost

sensors have been used to inform exposure risks in different applications including environmental justice(Kramer et al., 2023; Lu et al., 2022), wildfire exposure (Kramer et al., 2023), traffic-related exposure (Lu et al., 2022), and indoor exposure (Bi et al., 2021; Lu et al., 2022). The dense monitoring network enabled by deploying low-cost sensors provides the potential to understand the $PM_{2.5}$ exposure risk at a greater spatial and temporal resolution than the established regulatory air quality monitoring system. Federal Reference Method or Federal Equivalence Method (FRM/FEM) monitors tend to be sparsely sited due to the cost and complexity of this instrumentation.

Several studies have evaluated low-cost PM sensor performance for different sources and meteorological conditions, with bias and low precision reported in several cases (Ardon-Dryer et al., 2020; Barkjohn et al., 2021; Bi et al., 2020, 2021; He et al., 2020; Holder et al., 2020; Jayaratne et al., 2018; Kelly et al., 2017; Kim et al., 2019; Magi et al., 2020; Malings et al., 2020; Sayahi et al., 2019; Stavroulas et al., 2020; Tryner et al., 2020; Wallace et al., 2021). A study conducted in 2016 (AQ-SPEC, 2016), evaluating about twelve low-cost $PM_{2.5}$ sensors showed an overall good agreement between $PM_{2.5}$ PurpleAir sensors and two reference monitors with a R^2 of 78 % and 90 % (Wallace et al., 2021). However, an overestimation of 40 % was found for PurpleAir $PM_{2.5}$ concentrations[18,28.] Humidity has been documented as an important parameter that could greatly reduce the performance of the low-cost sensors (Rueda et al., 2023; Wallace et al., 2021; Zusman et al., 2020). Most low-cost PM sensors, including the PurpleAir sensor, utilize optical sensors to estimate PM mass from scattered light. Thus, they are subject to measurement errors from various factors, including particle size, composition, optical properties, and interactions of particles with atmospheric water vapor (Hagan & Kroll, 2020; Rueda et al., 2023; Zheng et al., 2018; Zusman et al., 2020). In a high humidity environment, accurate detection of particle size and concentration may be affected by hygroscopic particle growth (Carrico et al., 2010; L. Chen et al., 2022; Healy et al., 2014; Jamriska et al., 2008; Wallace et al., 2021). Water vapor may also damage the circuitry (Jamriska et al., 2008; Wallace et al., 2021). Relative Humidity (RH) has therefore been confirmed to be a principal source of measurement error that requires concentration correction in low-cost PM sensors (Barkjohn et al., 2021; Sayahi et al., 2019; Wallace et al., 2021; Zusman et al., 2020).

The PurpleAir PM sensor is one of the most commonly used low-cost PM sensors (Bi et al., 2021; Wallace et al., 2021). As of April 2022, there were more than 30,000 networked PurpleAir sensors, providing geolocated real-time air quality information (https://www2.purpleair.com, https://www.airnow.gov). Recently, the U.S. Environmental Protection Agency (EPA), after an evaluation of the sensors, developed a national correction model for PurpleAir sensors (Barkjohn et al., 2021). However, this evaluation included few sites in the Southeastern U.S. (Barkjohn et al., 2021).The study covered 16 states using 39 sites selected according to their collocation with an FRM/FEM monitor. In this study, the Southeastern U.S., the most humid region of the U.S., characterized by a humid subtropical climate(Konrad et al., 2013), was represented by only 5 sites and encompassed 4 states. The EPA correction model used multi-linear regression (MLR) (Barkjohn et al., 2021). Some recent studies used a model-based clusters (MBC) to improve performance metrics compared with their MLR models. McFarlane et al. (McFarlane et al., 2021) and Raheja et al. (Raheja et al., 2023) applied a Gaussian Mixture Regression (GMR) bias

correction model to PM$_{2.5}$ PurpleAir sensors in Accra, Ghana. The GMR-based model developed by McFarlane et al. (McFarlane et al., 2021) used daily data from one PurpleAir sensor collocated with one Met One Beta Attenuation Monitor 1020 from March 2020 to March 2021. Raheja et al. (Raheja et al., 2023) used 3 different low-cost sensors including PurpleAir PA-II collocated with a Teledyne T640 as the reference monitor at the University of Ghana, in Accra, Ghana, from May to September 2021. However, since the regression function in a GMR is derived from the joint probability of the data (Maugis et al., 2009; McFarlane et al., 2021; Shi & Choi, 2011), the GMR is not transferable to new settings (Raheja et al., 2023). The model is therefore not flexible enough to handle differences in proportions of the input variables observed at different locations.

The objective of our study is to develop and evaluate PurpleAir correction models for use in the warm humid climate zones (2A and 3A) in the U.S. (Antonopoulos et al., 2022) . First, we tested an MLR with different combinations of predictive variables. To avoid the transferability constraints observed for the GMR, our study then tested a novel semi-supervised clustering method. We used PurpleAir data and the FRM/FEM PM$_{2.5}$ data from the EPA Air Quality System (AQS) database from January 2021 to August 2023. We tested new correction models and compared them with the EPA nationwide PA data correction model proposed by Barkjohn et al. (Barkjohn et al., 2021) for the high-humidity Southeastern region of the country.

2 Methods

2.1 Study area

The study area includes the "warm-humid and moist" climate zone of the United States, as defined by the International Energy Conservation Code (EICC) in 2021 (Antonopoulos et al., 2022). The climate zone map comprises eight regions at county level, with seven represented in the continental U.S. (Antonopoulos et al., 2022; International Energy Conservation Code, 2021).The thermal climate zones are based on meteorological parameters (designated as 1 to 8) including precipitation, temperature, and humidity and a moisture regime (designated as A, B, C for Humid/Moist, Dry, and Marine respectively) based on monthly average temperature and precipitation (Antonopoulos et al., 2022; International Energy Conservation Code, 2021).

The study area was composed of climate zones and moisture regimes 2A and 3A. The "warm-humid" climate zone designation corresponds to a specific area of the climate zone map that includes Zones 2A and 3A (Fig. 1). Zone 1A is excluded, given that its tropical characteristics are sufficiently different from most of the Southeast. A warm and humid climate is characterized by high levels of humidity and high temperatures throughout the year and receives more than 20 inches (50 cm) of precipitation per year (Baechler et al., 2015). This area presents a state average annual humidity varying between 65.5 and 74.0 % and an average temperature per state varying between 55.1 and 70.7° F. These 12 states have the12 highest annual average dewpoint temperatures in the Continental U.S.

The study area includes 799 counties distributed into the 12 states as shown in the table in Fig. 1. Excepting Kentucky, all of the Southeastern U.S. states are partially or entirely characterized by a warm-humid climate zone and included in our study area.
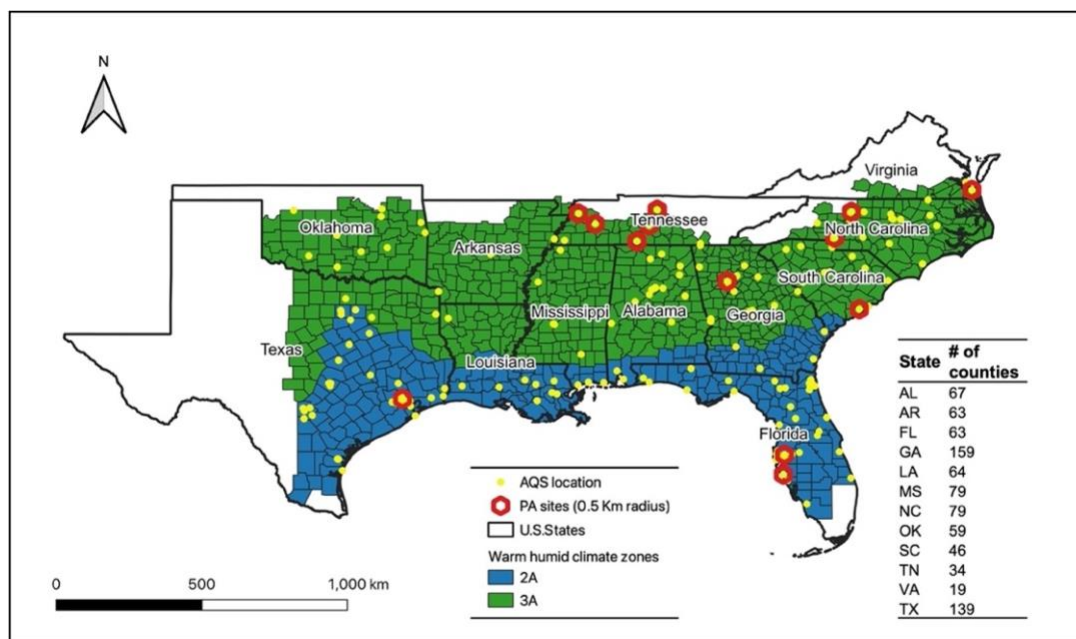
Figure 1: Study area showing the warm humid climate zones classification. The map also shows the distribution of available AQS monitors and the distribution of the PurpleAir sensors located at 0.5-km radius of an AQS monitor.

2.2 Data collection

The PurpleAir (PA-II-SD) contains two Plantower PMS5003 particle sensors; a sensor for pressure, temperature, and relative humidity (BME280); and a Wi-Fi module (Magi et al., 2020). $PM_{2.5}$ data from the PurpleAir sensors were obtained from the PurpleAir data repository (API PurpleAir. https://api.purpleair.com), and $PM_{2.5}$ data from the State and Local Air Monitoring System (SLAMS) were retrieved from the U.S. Environmental Protection Agency (EPA) Air Quality System (AQS) (U.S. EPA, 2023) for the period from 1 January 2021 to 28 August 2023 using their respective application programming interfaces (API). To obtain data for the study area, we used a bounding box (-100.01º W, -75.50º E and 25.81º S, 37.01º N) to find all outdoor sensors available for this geographical area. We identified 997 available sensors. We used the $PM_{2.5}$ dataset related to a standard environment, which was reported in the PurpleAir output as cf_1 (correction factor = 1). This represents a more appropriate raw measurement of PM concentrations without any nonlinear transformation (McFarlane et al., 2021), and has been used for several other studies (Barkjohn et al., 2021; Raheja et al., 2023; Tryner et al., 2020; Wallace et al., 2021). Hourly average $PM_{2.5}$ concentrations were downloaded for both PurpleAir sensors and AQS monitors.

SLAMS data are collected by local, state, and tribal government agencies and made available through the AirNow API (U.S. Environmental Protection Agency, 2023a). To ensure data accuracy, AQS data are collected by FRM or FEM monitors (U.S. Environmental Protection Agency, 2023b). These methods are primarily used to evaluate compliance with the National Ambient Air Quality Standards (NAAQS), although the data are often used for air pollution exposure and epidemiology

120   research. We identified 181 FEM or FRM monitors in our study area.

2.3 Selection of PurpleAir sensors and data quality control criteria

We selected PurpleAir sensors within fixed radii of each FRM or FEM monitor. The R Statistical Software (version R 4.3.1) was employed for data selection, data quality control, and statistical modeling. We identified outdoor PurpleAir sensors within 2.0, 1.0, and 0.5 km of each FRM or FEM monitor. When a PurpleAir sensor fell within the buffers of 2 or more AQS

125   monitors, the shorter distance to the AQS buffer centroid was applied to ensure better spatial join accuracy.

We applied a series of data exclusion criteria for quality control. First, we used a method detection limit of 1.5 $\mu g\ m^{-3}$ for the PurpleAir data. Wallace et al. (Wallace et al., 2021) calculated limits of detection ranging from 1.15 to 2.55 for the PurpleAir sensors (cf_1 data correction) in different cities. We also excluded all $PM_{2.5}$ data points that were greater than 1000 $\mu g\ m^{-3}$.

130   Then, we applied data exclusion criteria to clean the PurpleAir data based on agreement between the concentrations reported for the two sensors provided in the PurpleAir housing, labeled as Channels A and B. We considered low and high concentrations separately. For low $PM_{2.5}$ concentrations (less than or equal to 25 $\mu g\ m^{-3}$), we removed observations where the concentration difference between Channels A and B was greater than 5 $\mu g\ m^{-3}$ and the percent error deviation was greater than 20 %. For high $PM_{2.5}$ concentrations (greater than 25 $\mu g\ m^{-3}$), we removed data records when the percent error deviation

135   between Channels A and B was greater than 20 %. Similar cleaning criteria were used for quality assurance by Barkjohn et al. (Barkjohn et al., 2021) and Tryner et al. (Tryner et al., 2020), where data with a difference in concentration between Channels A and B was less than 5 $\mu g\ m^{-3}$ for low $PM_{2.5}$ concentration were considered valid. Bi et al. (Bi et al., 2020) removed data with the 5 % largest percent error difference between Channels A and B. Additionally, Barkjohn et al. (Barkjohn et al., 2021) excluded data points where Channels A and B that deviated by more than 61 %. However, we decided to employ a more

140   stringent criterion for our high concentration data records (20 % deviation) considering that our study only included reported PurpleAir data available via the API and only for one region of the United States. Following data cleaning, the final PurpleAir concentration (C_{PA}) dataset used in our study was obtained by averaging Channels A and B and included only hourly average PurpleAir data points that had a spatial (within the calculated radius) correspondence to hourly FRM or FEM concentration (C_{AQS}) data. Missing C_{AQS} data points were excluded before applying the radius-related spatial join.

145

To ensure data quality, the relative humidity measured by the BME280 sensor within the PurpleAir housing was evaluated. We compared hourly RH from the PurpleAir with the corresponding hourly RH from the National Oceanic and Atmospheric

Administration (NOAA) database. The NOAA data were downloaded using the R package worldmet (Carslaw, 2023). The nearest NOAA station to each PurpleAir sensor was considered for the comparison. The average distance between a NOAA

150   station and a PurpleAir sensor was approximately 10 miles with a minimum of 1.65 miles and a maximum of 25.50 miles. All the PurpleAir sensors that presented a correlation of less than 0.80 with the corresponding RH from NOAA were excluded.

2.4 Model correction

2.4.1 Model inputs

Because of the constraints related to water uptake (Hagan & Kroll, 2020; Rueda et al., 2023; Wallace et al., 2021), the most

155   commonly parameters found in the literature (Ardon-Dryer et al., 2020; Bi et al., 2020; Magi et al., 2020; Malings et al., 2020; Wallace et al., 2021), and used for correction of bias in $PM_{2.5}$ concentrations calculated from the PurpleAir are Temperature (T) and Relative Humidity (RH). Thus, our meteorological data (hourly T, hourly RH) were taken from the PurpleAir sensor, similar to the analysis conducted by Barkjohn et al. (Barkjohn et al., 2021). Barkjohn et al. (Barkjohn et al., 2021) included dewpoint temperature (DP) in addition to T and RH as an input predictor in their modeling process. However, DP was excluded

160   as a predictor in our study, because collinearity was found between DP, RH, and T when testing for variance inflation factor. This collinearity is attributed to the direct physical relationship between RH and T. For data quality assurance, we only included data records within a range of 0-130 ºF for T and 0-100 % for RH, respectively. Similar quality assurance criteria were employed by Wallace et al. (Wallace et al., 2021), where we removed data records with anomalous temperature and relative humidity.

165

The final dataset used for our model calibration included C_{PA}, C_{AQS}, RH, and T. We tested several multilinear regression models, and we defined a supervised clustering approach.

2.4.2 Multilinear Regression

Our study tested five Multilinear Regression (MLR) models (Equations 1-5) including the model proposed by Barkjohn et al.

170   (Barkjohn et al., 2021) (Model Bj). The models were structured as follows:

Model 1: $C_{AQS} = \beta_0 + \beta_1\, C_{PA} + \varepsilon$ (1)

Model 2: $C_{AQS} = \beta_0 + \beta_1\, C_{PA} + \beta_2\, RH + \varepsilon$ (2)

Model 3: $C_{AQS} = \beta_0 + \beta_1\, C_{PA} + \beta_2\, T + \varepsilon$ (3)

Model 4: $C_{AQS} = \beta_0 + \beta_1\, C_{PA} + \beta_2\, RH + \beta_3\, T + \varepsilon$ (4)

175   Model Bj: C_{AQS}[1]$= 5.72 + 0.524* C_{PA} - 0.0852*RH$ (5)

2.4.3 Semi-supervised Clustering

Alternative bias correction methods to MLR have been developed (Bi et al., 2020; McFarlane et al., 2021; Raheja et al., 2023) to capture complex nonlinear hygroscopic growth of particles (Hagan & Kroll, 2020; Rueda et al., 2023). Some of these alternative techniques include model-based clusters (MBC) (McFarlane et al., 2021; Raheja et al., 2023). An MBC assumes
180   that the data are composed of more than one subpopulations (Raftery & Dean, 2006). The influence of RH on PM$_{2.5}$ PurpleAir measurements, specifically at high ambient RH (Wallace et al., 2021), may be non-linear, suggesting formation of subgroups in our dataset. Therefore, our study tested a semi-supervised clustering (SSC) approach that combines unsupervised and supervised clustering processes to develop a non-linear MBC (Raftery & Dean, 2006). Before implementing the SSC, we carried out two pre-processing steps. The first pre-processing step consisted of finding the optimal predictors for the clusters
185   by applying a Gaussian Mixture Model (GMM) variable selection function (forward-backward) for MBC (Raftery & Dean, 2006). The optimal variables are then selected using the Bayesian information criterion (BIC). The list of potential variables included RH and T (the variable DP was excluded in this process because of multicollinearity with RH and T). The second pre-processing step was to optimize the number of clusters. For this, we used a combination of 26 clustering methods via the NbClust R package (Boehmke & Greenwell, 2019; Charrad et al., 2014). Knowing the optimal variable predictors and number
190   of clusters, we initiated the unsupervised portion of our SSC using the K-means clustering algorithm to derive the cluster. K-means, one of the most commonly employed clustering methods, is an unsupervised machine learning partitioning distance-based algorithm that computes the total within-cluster variation as the sum of squared (SS) Euclidian distances between the centroid of a cluster C_k and an observation x_i based on the Hartigan-Wong algorithm (Hartigan & Wong, 1979; Yuan & Yang, 2019). Last, we applied a supervised clustering process built upon the results obtained for the unsupervised clustering approach.
195   The supervised process allowed for distribution of the dataset within well-defined subsets. For each subset of the dataset associated with a cluster, an MLR was developed, defining a non-linear MBC (Equation 6).

$$y = \begin{cases} \beta_0 + \beta_1 x_{i1 \in C_1} + \cdots + \beta_p x_{ip \in C_1} + \in \\ \beta_0 + \beta_1 x_{i1 \in C_k} + \cdots + \beta_p x_{ip \in C_k} + \in \end{cases} \qquad (6)$$

200   where C_k is the number k of clusters regrouping x_i observations for each p explanatory variable.

---

[1] C_{AQS} here represents the reference PM$_{2.5}$ monitors used in Barkjohn et al. (2021).

2.4.4 Model validation

For each of the evaluated models, the coefficient of determination, R^2, was calculated to understand how well the regression model performs with the selected predictors. The predictive performance of each model was evaluated by estimating Root Mean Square Error (RMSE) and Mean Absolute Error (MAE). RMSE is defined as the standard deviation of the prediction errors. MAE measures the mean absolute difference between the modeled and the actual values. Standard deviation (SD), R^2 and RMSE are EPA's recommended performance metrics to evaluate a sensor's precision, linearity and uncertainty respectively (Duvall et al., 2021). We compared EPA's target value for SD, which refers to collocated identical sensors, with the estimated mean deviation or MAE for each paired observation of C_{AQS} and C_{PA}.

2.4.5 Cross-validation

Similar to Barkjohn et al. (Barkjohn et al., 2021), we used leave-one-group-out (LGOCV) cross-validation methods to evaluate how the model performs for an independent test dataset. LGOCV involves splitting the dataset into specific or random groups, then predicting each group as testing data with the other groups used for training. We used an automatic LGOCV, in which a random set of training data was composed to predict $PM_{2.5}$ concentrations at each iteration. An 80/20 ratio was defined between the training and test groups with 25 iterations. We used R^2, RMSE, and MAE as performance metrics to evaluate the cross-validation results.

2.4.6 Sensitivity analysis

Sensitivity analyses were performed to determine how predictions of $PM_{2.5}$ concentrations would vary under different temporal resolution. The sensitivity analysis applied the models, developed from hourly data at 0.5-km, 1.0-km, and 2.0-km buffers, to daily averaged data for the same buffers. We applied a completeness criterion of 90 %, or 21 hours, following Barkjohn et al. (Barkjohn et al., 2021)

3 Results and Discussion

After applying all the quality assurance (QA) criteria to the raw datasets, we obtained 159,648 observations (18 PA sites), 238,047 observations (28 PA sites), and 394,010 observations (50 PA sites) for buffers of 0.5 km, 1.0 km, and 2.0 km respectively, all at hourly temporal resolution. The QA process removed 25-30 % of the raw data, with data from 3 PA sites completely removed for the 0.5-km radius because RH from the humidity sensors correlated poorly with RH reported by NOAA stations (Fig. S1). We found that two of these same 3 PA sites exhibited poor correlation for temperature as well. Moreover, the slope of the linear regression estimated for each PA sensor (Fig. 1) shows that RH from these 3 PA sites exhibited the larger bias metrics. All 18 retained PA sites presented RH data that strongly correlated with NOAA stations (88-96 %), with 16 of them presenting an R equal or greater than 90 % (Fig. S1). As reported by recent studies (Giordano et al., 2021; Lunden et al., 2022; Magi et al., 2020; Tryner et al., 2020), PurpleAir sensors tend to report dryer humidity measurements

than ambient conditions. The comparison of our PurpleAir sensors with NOAA stations showed that each of the 18 retained PA sites reported lower humidity measurements than their corresponding NOAA station. They presented a negative difference in RH varying between 10 %-20 %, with uncertainty increasing with increased RH (Fig. S2). In addition to the 3 PA sites removed for the 0.5-km radius, 1 and 2 additional PA sites were removed for the 1.0 km and 2.0 km buffers, respectively. We

235 did not detect any additional instrument error for temperature. Most of the retained PA sites had a strong correlation of 95-99 % for temperature with NOAA stations.
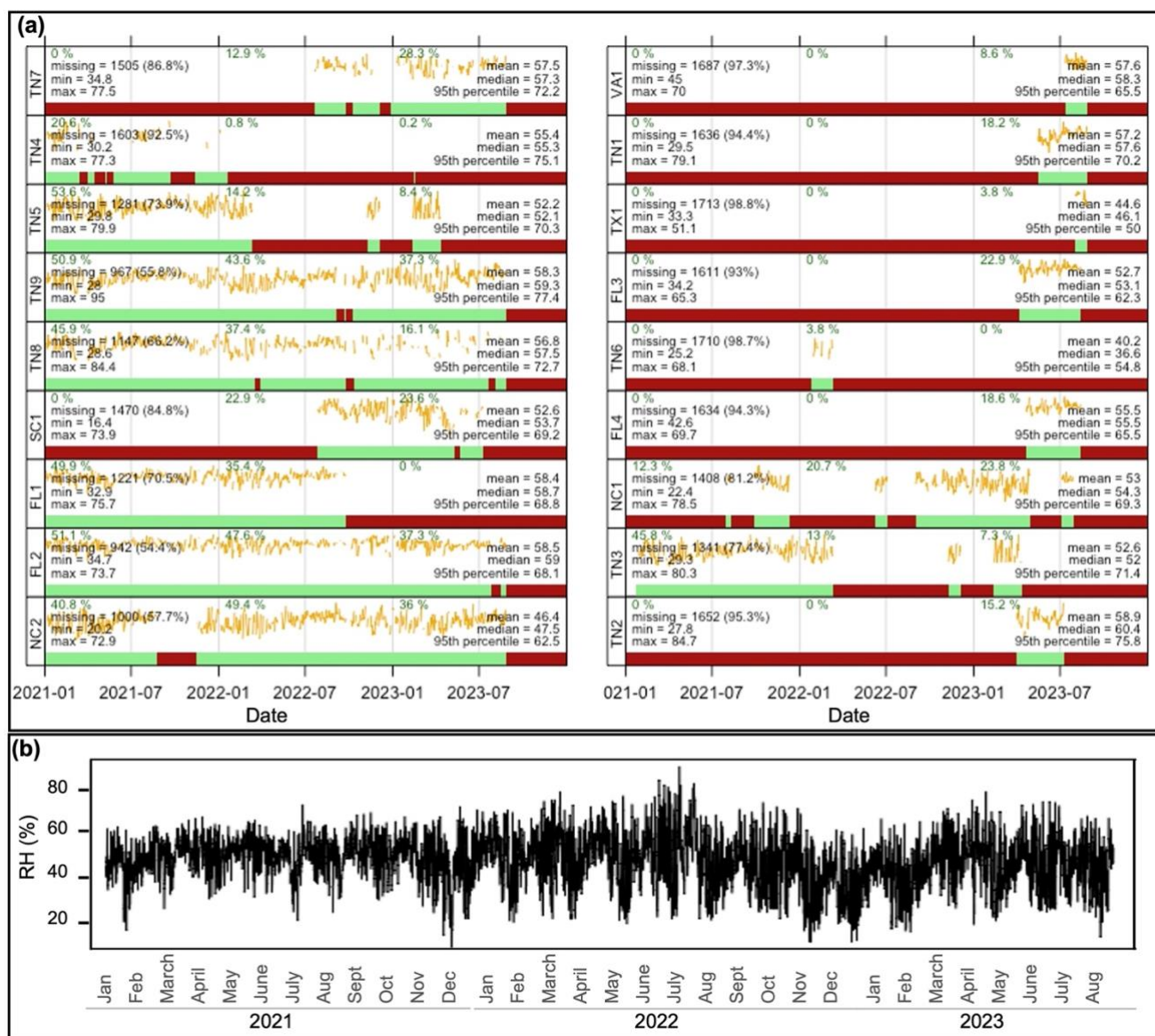

Figure 2: (a) Summary statistics and time series (yellow lines) of daily average RH for each PA site showing the presence of data (green) and missing data (red). The represent RH scaled from z to the maximum daily value. The percentage of data captured per

240 year is also provided. (b) Time series of daily average RH for the entire dataset.

Summary statistics were explored to describe the main characteristics of our datasets (Fig. 2 and 3). Meteorological parameters for our three buffers (0.5 km, 1.0 km and 2.0 km) exhibit roughly the same distribution (Fig. S3). Further evaluation of our 0.5-km radius dataset revealed that 63 % of the hourly data for RH are greater than 50 % with temperatures varying between

245 -17.13 and 38.83 °C. RH for the 0.5-km radius dataset showed some monthly seasonality (Fig. 2B). However, independent of the number of months of data reported by a PurpleAir sensor, the distribution of RH is relatively consistent for individual PA sites (Fig. 2A). For this same radius, the number of complete months of data per PA sensor varied from approximately 1 to 29 months, with 11 sensors covering at least 10 months of hourly data (Fig. 2A).

250 For the PM$_{2.5}$ concentration data, Fig. 2 displays the mean and SD for the C$_{AQS}$ and C$_{PA}$ data for all three analyzed buffers. The Pearson correlation (R), R^2, RMSE and MAE between C$_{AQS}$ and C$_{PA}$ before fitting any model were also estimated for each radius (Fig. 2). All of the metrics, R^2, MAE and RMSE exceeded the target values[2] (R$^2 \geq$ 70 %, SD $\leq$ 5 µg m^{-3} and RMSE $\leq$ 7 µg m^{-3}) recommended by EPA(Duvall et al., 2021). Raw C$_{PA}$ presented greater magnitude and variability than C$_{AQS}$ (Fig. 2). The performance metrics (Tables 1 and 2, Tables S1-S4) indicated less error with successively smaller buffer size, which

255 suggests that model fit improved as the distance between the AQS monitors and PA sensors decreased. The distance factor might be attributed with spatial variability between AQS monitors and PA sensors and the effect of various potential PM sources around the air monitors. Therefore, we present only the results for the 0.5-km buffer analysis. Tables S1-S4 contain the results for the 1.0-km and 2.0-km buffers, respectively. Wallace et al. (Wallace et al., 2021) and Bi et al. (Bi et al., 2021) also used a 0.5-km buffer around the AQS monitors in their low-cost sensor data calibration studies.
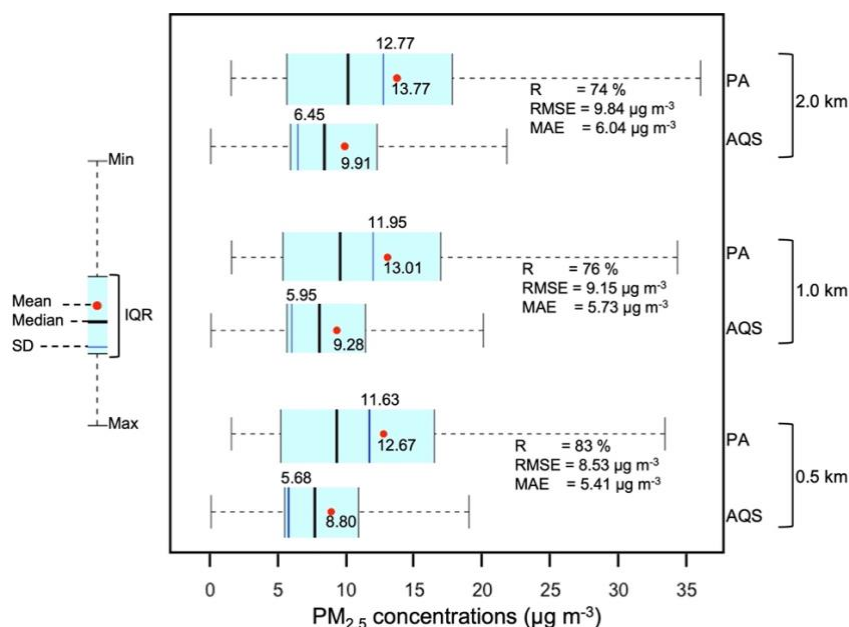

260

Figure 3: Descriptive and error metrics for C_{AQS} and raw C_{PA} for PurpleAir sensors within a 0.5-km, 1.0-km and 2.0-km radii of each FRM or FEM monitor.

3.1 MLR Bias-Correction Model

The bias-correction models, including the Barkjohn model (Barkjohn et al., 2021), and their performance metrics are presented
265 in Table 1. Our dataset illustrates improved predictive performance for our four MLR-fitted models compared with the
Barkjohn model (Table 1). The Barkjohn model presented a higher R^2, as a measure of the goodness of fit, than Model 1,
however Model 1 is improved with respect to all error metrics. RMSE and MAE, which summarize the error on hourly $PM_{2.5}$
averages, exhibited relatively low values for the four models when we consider the average C_{AQS} in the dataset and its SD, and
the EPA's target value[2] (≤ 7 µg m^{-3}) for RMSE. The best model fit was observed for Model 4, incorporating C_{PA}, T, and RH,
270 with substantially improved prediction metrics over the other models (Table 1). For all the four fitted models, average
concentration of 8.80 µg m^{-3}, with an SD varying between 4.71- 4.84 µg m^{-3} were obtained, whereas Model Bj provided and a
higher MAE than the four developed models with a mean of 7.67 µg m^{-3} and a SD of 6.08 µg m^{-3}. Furthermore, unlike our
fitted models, Model Bj applied to our dataset displayed some negative values. Model 2 was similar in structure to the selected
model from Barkjohn et al. (Barkjohn et al., 2021), with C_{PA} and RH as predictors. All predictors for every model were
275 statistically significant. Validation testing using the LGOCV (Table S5) presented nearly identical results to models using the
entire dataset, building confidence in the models.

Our findings align with some previous low-cost sensor data calibration work (Barkjohn et al., 2021; Magi et al., 2020; Zheng
et al., 2018), where relatively simple calibration models provided reasonable bias correction. Zheng et al. (Zheng et al., 2018)
280 found an R^2 value of 66 % for a 1-h averaging period after applying an MLR calibration equation to compare three PA sensors
against each other and a co-located reference monitor over a period of 30 days. A study conducted by Magi et al. (Magi et al.,
2020), involving a sixteen-month PurpleAir $PM_{2.5}$ data collection in an urban setting in Charlotte, North Carolina, resulted in
R^2 of 60 % for an MLR including C_{PA}, RH and T. Barkjohn et al. (Barkjohn et al., 2021) estimated an RMSE of 3 µg m^{-3} (no
decimal specified) when fitting a model with RH for an average concentration of 9 µg m^{-3} for FRM or FEM monitors.
285 Moreover, the negative coefficient obtained for RH for Model 2 and Model 4 is not surprising considering that high RH can
lead to hygroscopic growth of the particles, and therefore cause uncertainties and overestimation in PurpleAir $PM_{2.5}$
concentration readings (Bi et al., 2021; Wallace et al., 2021). The model developed by Barkjohn et al. (Barkjohn et al., 2021),
as well as the MLR model developed by Raheja et al. (Raheja et al., 2023) using data in Accra, Ghana, had a negative
coefficient for RH.
290

Table 1: MLR model development (model fit using hourly data) and application of the hourly model to daily data.

Parameters	Model fit with hourly data				Model fit to daily data			
Models	R^2 (%)	RMSE (µg m^{-3})	MAE (µg m^{-3})	R (%)	R^2 (%)	RMSE (µg m^{-3})	MAE (µg m^{-3})	R (%)

Model 1	$3.6667550 + 0.4053418PA_i$	69	3.16	2.13	83	76	2.39	1.67	87
Model 2	$6.3384228 + 0.4143437PA_i - 0.0506037RH_i$	71	3.05	2.05	84	76	2.35	1.64	87
Model 3	$1.7642336 + 0.4109897PA_i + 0.0847196T_i$	71	3.04	2.06	84	77	2.32	1.67	88
Model 4	$4.3295358 + 0.4182906PA_i - 0.0445768RH_i + 0.0752867T_i$	73	2.96	1.99	85	79	2.24	1.59	89
Model Bj	$5.72 + 0.524PA_i - 0.0852RH_i$	71	3.52	2.51	84	76	2.76	2.06	87

Following removal of datapoints that did not fit the QA criteria, the 0.5-km daily dataset included 5,666 observations for the same 18 sensors when applying the hourly model to daily data. These produced a substantial improvement in the performance

295   metrics compared with the hourly models (Table 1). Model 4 presented better performance metrics compared to the other models (Table 1). Figure 4 shows the correlation between the predicted C_{PA} and C_{AQS} for Model 4 and Model Bj along with the distribution of RH. The Barkjohn et al. model (Barkjohn et al., 2021) used only daily averaged data, thus, it was directly comparable with our application of the model to daily data. An evaluation of Model Bj applied to our warm-humid climate zone daily PA datasets revealed substantially higher error metrics than the other models (Table 1) with an SD of 5.14 $\mu g\ m^{-3}$.
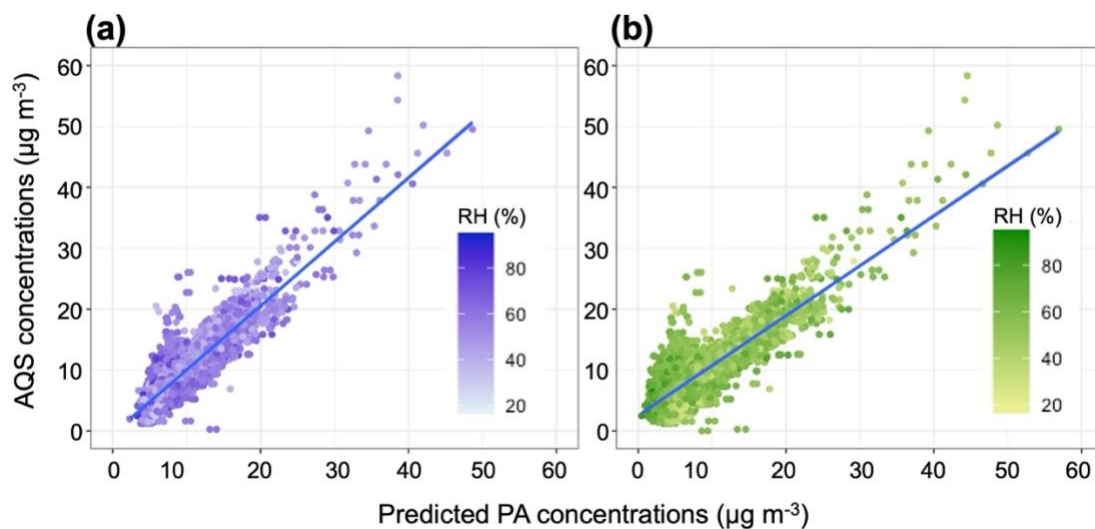
300

Figure 4: Positive linear correlation between daily AQS and daily predicted PM$_{2.5}$ concentrations with RH distribution using Model 4 (a) and the Barkjohn model (b) of the MLR process.

3.2 SSC Model Predictions

The SSC model included the same predictors as Model 4 (C_{PA}, RH and T) as the best MLR model obtained. The GMM process,
305 discerning complex relationships between variables, found that RH and T are optimal predictors to use in the clustering process.
Among the twenty-six indices evaluated, we found that eight of them proposed k=2 as the optimal number of clusters (Table
S7). Thus, we set k=2 clusters for the unsupervised aspect of our SSC process. Figure 5A shows the k clusters result for the
silhouette algorithm, which is based on two factors, cohesion (similarity of an object with a cluster) and separation (comparison
among clusters) (Yuan & Yang, 2019). The unsupervised clustering suggested a distribution of the dataset into two well-
310 defined clusters based on the RH predictor (Fig. 5B). For T, the same range of values was found within each defined cluster.
RH, being the most important variable that determined the clustering subdivision (Fig. 5B), therefore, we considered only RH
for the cluster subdivision and then we applied the supervised phase of the SSC process to adjust the random subdivision of
the clusters and eliminate overlaps. The 2 clusters were RH ≤ 50 % (Cluster 1) and RH > 50 % (Cluster 2) (Table 2). This
result aligns with Wallace et al. (Wallace et al., 2021), showing that the nonlinear effect between $PM_{2.5}$ and RH emerges around
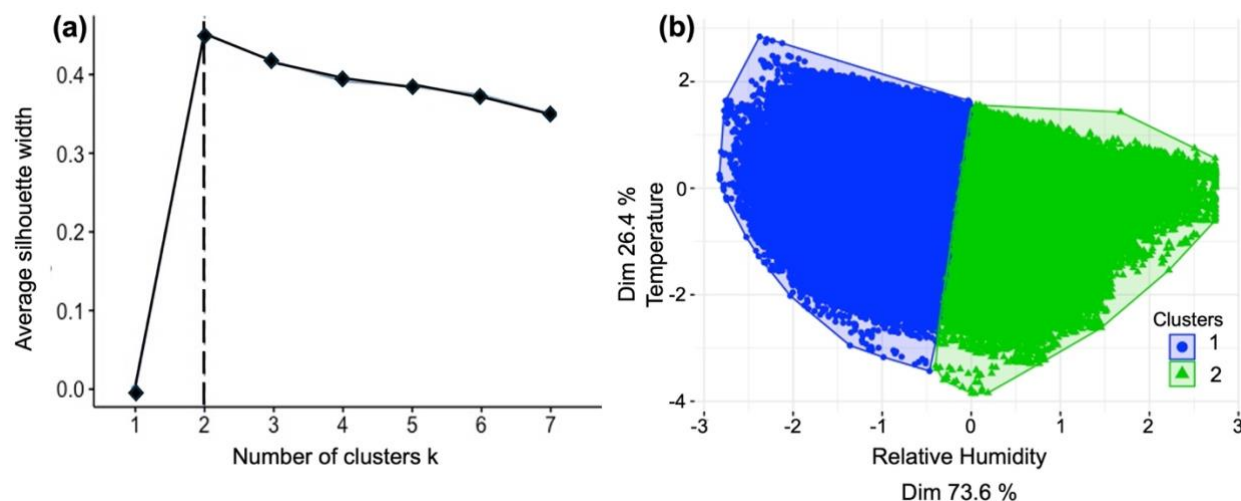315 a RH of 50 %, similar to our cluster division.

Figure 5: Unsupervised clustering results: (a) Number of clusters k using the silhouette algorithm; (b) Clustering subsets based on RH and T showing that RH has a greater influence in the process. The axis values correspond to covariance, and the dimensionality corresponds to how much of each variable participated in the clustering process.

320 The SSC approach provides improved model fits compared with the MLR models for our hourly data. Table 2 presents the
modeling results of the RH-based semi-supervised clustering process. All predictors were statistically significant. Models from
both clusters are within the range of the EPA's target values for linearity and error performance metrics (Table 2). Except for
MAE that is much lower for Cluster 1, Cluster 2 model presented better performance metrics compared with the Cluster 1
model (Table 2). Compared with Model 4 from the MLR models, results from Cluster 1 showed equal RMSE and a very low
325 MAE, while estimated metrics from Cluster 2 are greatly improved with the exception of MAE (Table 2). The combined

predicted PA concentrations from the two SSC clusters resulted in an RMSE of 2.94 µg m^{-3} and a MAE of 1.96 µg m^{-3}. Similar to the MLR validation testing, LGOCV for SSC (Table S6) produced similar MAEs compared with the models using the entire dataset. Thus, the cluster-based models may be valid for any individual PA sensors in the study area.

330 The previous studies(McFarlane et al., 2021; Raheja et al., 2023) using an MBC to calibrate low-cost sensors are consistent with our SSC results with lower MAEs/RMSEs for their GMR-based model compared with their MLR, indicating that an MBC is superior to an MLR approach. McFarlane et al. (McFarlane et al., 2021) in their studies found for their GMR model a MAE of 0.5 less for their MLR of 2.2 µg m^{-3}. Similarly, Raheja et al. (Raheja et al., 2023), for their GMR model using PA sensors, found a MAE of 1.93 µg m^{-3} and a RMSE of 2.58 µg m^{-3}, corresponding to 0.17 µg m^{-3} and 0.30 µg m^{-3} less than their
335 MLR model respectively. However, because of transferability (Raheja et al., 2023) constraints with GMR-based models, Raheja et al. (Raheja et al., 2023), recommended to use their MLR model for future applications, although they obtained an improved model using the GMR.

Table 2: Semi-supervised clustering model development (model fit with hourly data) and application of the hourly model to
340 daily data.

Parameters		Model fit with hourly data				Model fit to daily data			
Clusters (Number of observations)	Models	R^2 (%)	RMSE (µg m^{-3})	MAE (µg m^{-3})	R (%)	R^2 (%)	RMSE (µg m^{-3})	MAE (µg m^{-3})	R (%)
RH ≤ 50 (59405)	2.738732 + 0.425834 PA$_i$ - 0.008944 RH$_i$ + 0.079210 T$_i$	71	2.96	1.86	84	88	2.04	1.46	94
RH >50 (100243)	7.230374 + 0.412683 PA$_i$ - 0.085278 RH$_i$ + 0.070655 T$_i$	74	2.92	2.02	86	73	2.33	1.68	85

As for the MLR, the SSC hourly model was applied to the daily average dataset. Figure 6 shows the nonlinearity of our dataset with the slope varying for each cluster for the correlation between C$_{AQS}$ and C$_{PA}$. Applying the hourly models to daily data resulted in substantial improvement with lower uncertainties in each SSC model compared with the hourly dataset (Table 2).
345 Compared with the fit for Model 4 from the MLR (Table 1) to daily data, we observed that Cluster 1 presented better performance metrics than Cluster 2 (Tables 1 and 2). Compared with Model Bj applied to our daily dataset in Table 1, the daily SSC models display improved results (lower RMSE and MAE) for each cluster.
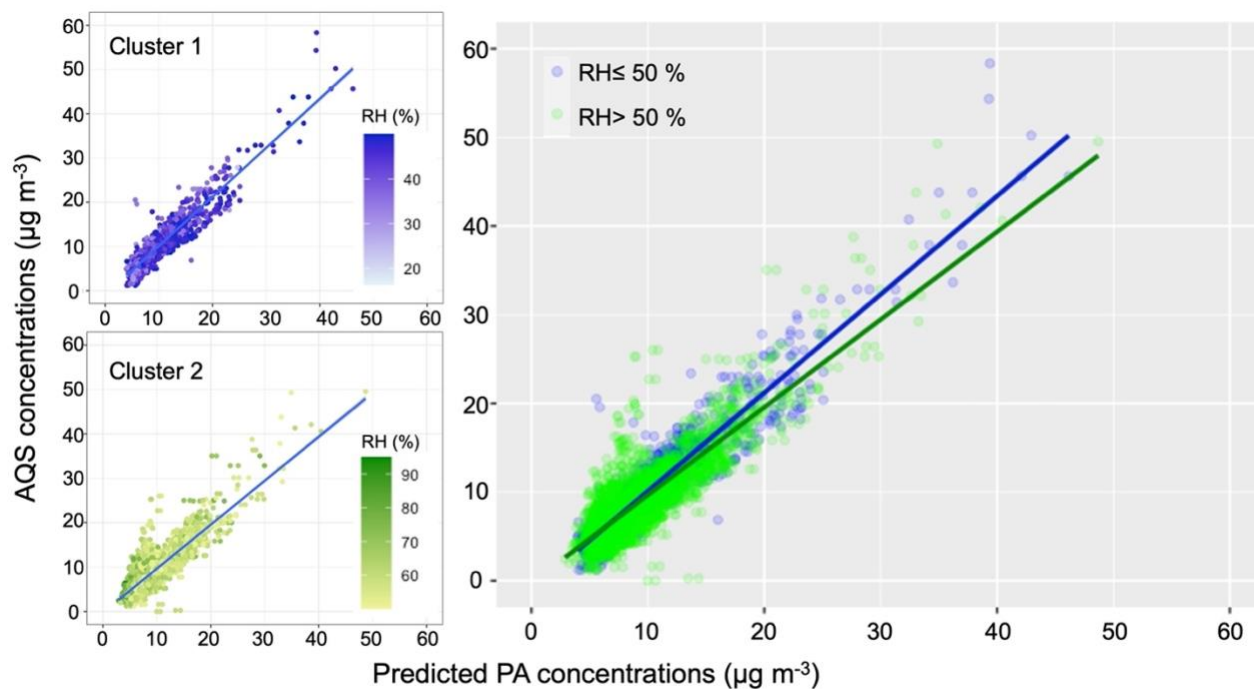
Figure 6: Correlation between daily AQS and daily predicted PM₂.₅ concentrations using the SSC model. Each cluster is presented
350 **separately on the left, and both clusters are shown on the right.**

To further assess the model performance in subgroups, Model 4 from the MLR and the SSC models were applied to daily data
from 5 states of the warm-humid climate zones (Table 3). For the SSC, both models presented good results for all the metrics
compared with the hourly-data-fitted models and their application to daily data. Except for VA, where Model 4 produced lower
error metric values, the SSC model outperformed the MLR for all the states.

355

Table 3: Application of MLR- Model 4 and SSC model to individual state. The SSC combined clusters result is the result
obtained after applying each cluster to the daily data, then added together.

States	MLR			SSC combined Clusters		
	RMSE (µg m⁻³)	MAE (µg m⁻³)	R (%)	RMSE (µg m⁻³)	MAE (µg m⁻³)	R (%)
SC	2.11	1.5	85	2.06	1.45	85
NC	2.81	1.82	89	2.76	1.76	90
VA	2.38	2.2	97	2.63	2.46	97
FL	2.63	1.64	81	2.58	1.62	81
TN	3.11	2.21	87	3.10	2.19	87

15

3.3 Final Model Selection
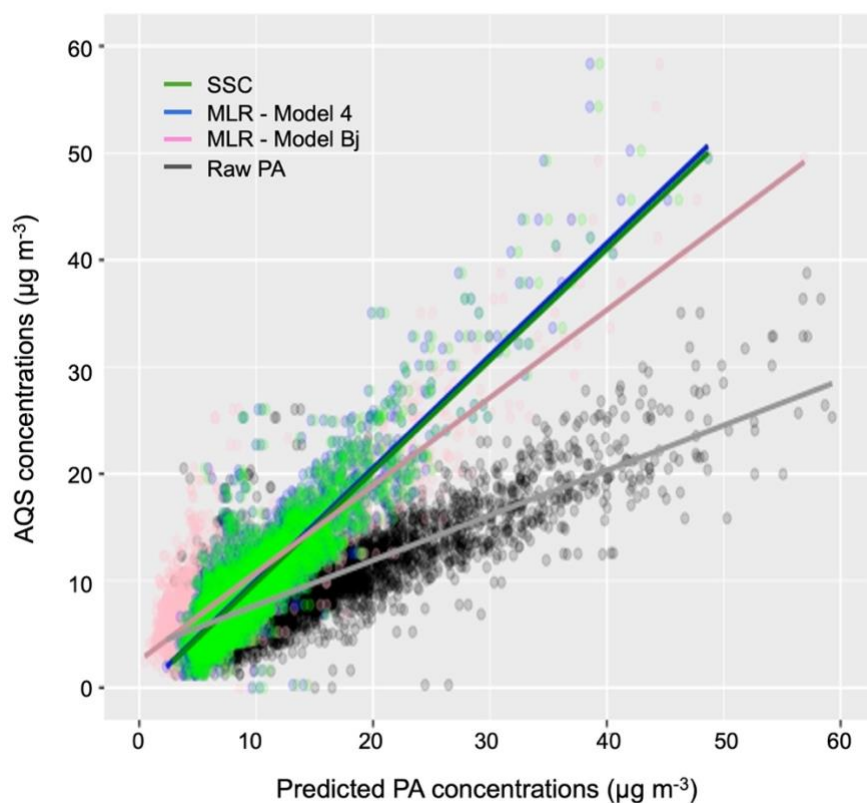
Figure 7: **Correlation between daily AQS and daily raw/predicted PM$_{2.5}$ concentrations using the MLR, the SSC and Model Bj.**

Both Model 4 from the MLR models and the SSC models align with previous studies, producing low error and high correlation R^2. We included in the supplemental information (Table S8) these two sets of models (Model 4 from the MLR models and the SSC models) using NOAA meteorological data for RH and T that can be applied when meteorological information from PA sensors is biased or missing. Figure 7 summarizes the results of our study by presenting the correlation fit for the MLR (Model 4 from the MLR models), the combined clusters from the SSC, the Model Bj and the raw PA data together. Our results showed that applying Model Bj to our hourly dataset improved our error metric, RMSE, of 58.73 % from the the raw data. The MLR and the SSC model have lower error and higher correlation than Model Bj. A decrease of 15.91 % was obtained for RMSE from Model Bj to Model 4. However, Model 4 PM$_{2.5}$ concentrations had a higher average mean deviation (1. 99 µg m^{-3}) from C$_{AQS}$ than PM$_{2.5}$ concentrations from the SSC model (1.96 µg m^{-3}). Moreover, Model 4 PM$_{2.5}$ concentrations from the MLR models tend to be slightly higher than PM$_{2.5}$ concentrations from the SSC model at high RH and slightly lower at lower RH.

4. Conclusion

In conclusion, Model 4 from the MLR and the SSC model improved the error performance metrics by 16-23 % compared with the Barkjohn et al. model (Barkjohn et al., 2021). The SSC model presented slightly better results than the overall MLR, suggesting that a clustering approach might be more accurate in areas with high humidity conditions to capture the non-linearity

375 associated with hygroscopic growth of particles in such conditions. Therefore, the SSC model is recommended to be used for bias correction for the Southeastern United States. However, Model 4 might be an acceptable alternative for its parsimony. Applying these models to $PM_{2.5}$ PurpleAir concentrations collected in high humidity areas will help to inform communities with a high-quality estimation of their exposure. These models might also benefit communities in high humidity regions outside of the U.S. Next steps in model development may include evaluation of the transferability of these models to other humid

380 locations in the world.

Code and data availability

All code and data will be made available through the Dryad Digital Repository.

Author contributions

385 MEM-C, AG and JR-B conceptualized the work and developed the methods. MEM-C curated the data, completed the formal analysis and figure visualizations. MEM-C and CG wrote the original draft. MEM-C, CG, AG and JR-B reviewed and edited the manuscript. JR-B acquired funding.

Competing interests

The authors declare that they have no conflict of interest.

References

395   Antonopoulos, C.; Gilbride, T.; Margiotta, E.; Kaltreider, C. *Guide to Determining Climate Zone by County: Building America and IECC 2021 Updates*; Richland, WA (United States), 2022. https://doi.org/10.2172/1893981.

API PurpleAir. https://www. api.purpleair.com.

AQ-SPEC. *http://www.aqmd.gov/docs/default-source/aq-spec/field-evalua tions/purpleair—field-evaluation.pdf.*

Ardon-Dryer, K.; Dryer, Y.; Williams, J. N.; Moghimi, N. Measurements of PM2.5 with PurpleAir under Atmospheric
400   Conditions. *Atmos Meas Tech* **2020**, *13* (10). https://doi.org/10.5194/amt-13-5441-2020.

Baechler, M. C.; Gilbride, T. L.; Cole, P. C.; Hefty, M. G.; Ruiz, K. *Guide to Determining Climate Regions by County*; 2015; Vol. 7.

Barkjohn, K. K.; Gantt, B.; Clements, A. L. Development and Application of a United States-Wide Correction for PM2.5 Data Collected with the PurpleAir Sensor. *Atmos Meas Tech* **2021**, *14* (6). https://doi.org/10.5194/amt-14-4617-2021.

405   Bi, J.; Wallace, L. A.; Sarnat, J. A.; Liu, Y. Characterizing Outdoor Infiltration and Indoor Contribution of PM2.5 with Citizen-Based Low-Cost Monitoring Data. *Environmental Pollution* **2021**, *276*, 116763. https://doi.org/10.1016/J.ENVPOL.2021.116763.

Bi, J.; Wildani, A.; Chang, H. H.; Liu, Y. Incorporating Low-Cost Sensor Measurements into High-Resolution PM2.5 Modeling at a Large Spatial Scale. *Environ Sci Technol* **2020**, *54* (4), 2152–2162. https://doi.org/10.1021/acs.est.9b06046.

410   Boehmke, B.; Greenwell, B. *Hands-On Machine Learning with R*; 2019. https://doi.org/10.1201/9780367816377.

Brook, R. D.; Rajagopalan, S.; Pope, C. A.; Brook, J. R.; Bhatnagar, A.; Diez-Roux, A. V.; Holguin, F.; Hong, Y.; Luepker, R. V.; Mittleman, M. A.; Peters, A.; Siscovick, D.; Smith, S. C.; Whitsel, L.; Kaufman, J. D. Particulate Matter Air Pollution and Cardiovascular Disease: An Update to the Scientific Statement from the American Heart Association. *Circulation*. 2010. https://doi.org/10.1161/CIR.0b013e3181dbece1.

415   Carrico, C. M.; Petters, M. D.; Kreidenweis, S. M.; Sullivan, A. P.; McMeeking, G. R.; Levin, E. J. T.; Engling, G.; Malm, W. C.; Collett, J. L. Water Uptake and Chemical Composition of Fresh Aerosols Generated in Open Burning of Biomass. *Atmos Chem Phys* **2010**, *10* (11), 5165–5178. https://doi.org/10.5194/acp-10-5165-2010.

Carslaw, D. *worldmet: Import Surface Meteorological Data from NOAA Integrated Surface Database (ISD)*. https://davidcarslaw.github.io/worldmet/index.html, http://davidcarslaw.github.io/worldmet/.

420   Charrad, M.; Ghazzali, N.; Boiteau, V.; Niknafs, A. Nbclust: An R Package for Determining the Relevant Number of Clusters in a Data Set. *J Stat Softw* **2014**, *61* (6). https://doi.org/10.18637/jss.v061.i06.

Chen, L. J.; Ho, Y. H.; Lee, H. C.; Wu, H. C.; Liu, H. M.; Hsieh, H. H.; Huang, Y. Te; Lung, S. C. C. An Open Framework for Participatory PM2.5 Monitoring in Smart Cities. *IEEE Access* **2017**, *5*. https://doi.org/10.1109/ACCESS.2017.2723919.

Chen, L.; Zhang, F.; Zhang, D.; Wang, X.; Song, W.; Liu, J.; Ren, J.; Jiang, S.; Li, X.; Li, Z. Measurement Report: Hygroscopic
425   Growth of Ambient Fine Particles Measured at Five Sites in China. *Atmos Chem Phys* **2022**, *22* (10). https://doi.org/10.5194/acp-22-6773-2022.

Chen, R.; Hu, B.; Liu, Y.; Xu, J.; Yang, G.; Xu, D.; Chen, C. Beyond PM2.5: The Role of Ultrafine Particles on Adverse Health Effects of Air Pollution. *Biochim Biophys Acta Gen Subj* **2016**, *1860* (12). https://doi.org/10.1016/j.bbagen.2016.03.019.

430   Cohen, A. J.; Brauer, M.; Burnett, R.; Anderson, H. R.; Frostad, J.; Estep, K.; Balakrishnan, K.; Brunekreef, B.; Dandona, L.; Dandona, R.; Feigin, V.; Freedman, G.; Hubbell, B.; Jobling, A.; Kan, H.; Knibbs, L.; Liu, Y.; Martin, R.; Morawska, L.; Pope, C. A.; Shin, H.; Straif, K.; Shaddick, G.; Thomas, M.; van Dingenen, R.; van Donkelaar, A.; Vos, T.; Murray, C. J. L.; Forouzanfar, M. H. Estimates and 25-Year Trends of the Global Burden of Disease Attributable to Ambient Air Pollution: An Analysis of Data from the Global Burden of Diseases Study 2015. *The Lancet* **2017**, *389* (10082).

435   https://doi.org/10.1016/S0140-6736(17)30505-6.

Duvall, R. M.; Clements, A. L.; Hagler, G.; Kamal, A.; Kilaru, V.; Goodman, L.; Frederick, S.; Barkjohn, K. K.; VonWald, I.; Greene, D.; Dye, T. *Performance Testing Protocols, Metrics, and Target Values for Fine Particulate Matter Air Sensors: Use in Ambient, Outdoor, Fixed Site, Non-Regulatory Supplemental and Informational Monitoring Applications*; 2021.

Giordano, M. R.; Malings, C.; Pandis, S. N.; Presto, A. A.; McNeill, V. F.; Westervelt, D. M.; Beekmann, M.; Subramanian,

440   R. From Low-Cost Sensors to High-Quality Data: A Summary of Challenges and Best Practices for Effectively Calibrating Low-Cost Particulate Matter Mass Sensors. *J Aerosol Sci* **2021**, *158*. https://doi.org/10.1016/j.jaerosci.2021.105833.

Hagan, D. H.; Kroll, J. H. Assessing the Accuracy of Low-Cost Optical Particle Sensors Using a Physics-Based Approach. *Atmos Meas Tech* **2020**, *13* (11). https://doi.org/10.5194/amt-13-6343-2020.

Hartigan, J. A.; Wong, M. A. Algorithm AS 136: A K-Means Clustering Algorithm. *Appl Stat* **1979**, *28* (1).

445   https://doi.org/10.2307/2346830.

He, M.; Kuerbanjiang, N.; Dhaniyala, S. Performance Characteristics of the Low-Cost Plantower PMS Optical Sensor. *Aerosol Science and Technology* **2020**, *54* (2). https://doi.org/10.1080/02786826.2019.1696015.

Health Effects Institute. *State of Global Air 2020. Special Report*; 2020.

Healy, R. M.; Evans, G. J.; Murphy, M.; Jurányi, Z.; Tritscher, T.; Laborde, M.; Weingartner, E.; Gysel, M.; Poulain, L.;

450   Kamilli, K. A.; Wiedensohler, A.; O'Connor, I. P.; McGillicuddy, E.; Sodeau, J. R.; Wenger, J. C. Predicting Hygroscopic Growth Using Single Particle Chemical Composition Estimates. *J Geophys Res* **2014**, *119* (15). https://doi.org/10.1002/2014JD021888.

Holder, A. L.; Mebust, A. K.; Maghran, L. A.; McGown, M. R.; Stewart, K. E.; Vallano, D. M.; Elleman, R. A.; Baker, K. R. Field Evaluation of Low-cost Particulate Matter Sensors for Measuring Wildfire Smoke. *Sensors (Switzerland)* **2020**, *20* (17).

455   https://doi.org/10.3390/s20174796.

International Energy Conservation Code. *Chapter 3, General requirements, 2021 International Energy Conservation Code (IECC)*. https://codes.iccsafe.org/content/IECC2021P2/chapter-3-re-general-requirements.

Jamriska, M.; Morawska, L.; Mergersen, K. The Effect of Temperature and Humidity on Size Segregated Traffic Exhaust Particle Emissions. *Atmos Environ* **2008**, *42* (10). https://doi.org/10.1016/j.atmosenv.2007.12.038.

460 Jayaratne, R.; Liu, X.; Thai, P.; Dunbabin, M.; Morawska, L. The Influence of Humidity on the Performance of a Low-Cost Air Particle Mass Sensor and the Effect of Atmospheric Fog. *Atmos Meas Tech* **2018**, *11* (8). https://doi.org/10.5194/amt-11-4883-2018.

Jiao, W.; Hagler, G.; Williams, R.; Sharpe, R.; Brown, R.; Garver, D.; Judge, R.; Caudill, M.; Rickard, J.; Davis, M.; Weinstock, L.; Zimmer-Dauphinee, S.; Buckley, K. Community Air Sensor Network (CAIRSENSE) Project: Evaluation of

465 Low-Cost Sensor Performance in a Suburban Environment in the Southeastern United States. *Atmos Meas Tech* **2016**, *9* (11). https://doi.org/10.5194/amt-9-5281-2016.

Kelly, K. E.; Whitaker, J.; Petty, A.; Widmer, C.; Dybwad, A.; Sleeth, D.; Martin, R.; Butterfield, A. Ambient and Laboratory Evaluation of a Low-Cost Particulate Matter Sensor. *Environmental Pollution* **2017**, *221*. https://doi.org/10.1016/j.envpol.2016.12.039.

470 Kim, S.; Park, S.; Lee, J. Evaluation of Performance of Inexpensive Laser Based PM2.5 Sensor Monitors for Typical Indoor and Outdoor Hotspots of South Korea. *Applied Sciences (Switzerland)* **2019**, *9* (9). https://doi.org/10.3390/app9091947.

Konrad, C. E.; Fuhrmann, C. M.; Billiot, A.; Keim, B. D.; Kruk, M. C.; Kunkel, K. E.; Needham, H.; Shafer, M.; Stevens, L. Climate of the Southeast USA: Past, Present, and Future. In *Climate of the southeast United States: Variability, change, impacts, and vulnerability* ; 2013; Vol. Washington, DC:, pp 8–42.

475 Kramer, A. L.; Liu, J.; Li, L.; Connolly, R.; Barbato, M.; Zhu, Y. Environmental Justice Analysis of Wildfire-Related PM2.5 Exposure Using Low-Cost Sensors in California. *Science of The Total Environment* **2023**, *856*, 159218. https://doi.org/10.1016/J.SCITOTENV.2022.159218.

Landrigan, P. J.; Fuller, R.; Acosta, N. J. R.; Adeyi, O.; Arnold, R.; Basu, N. (Nil); Baldé, A. B.; Bertollini, R.; Bose-O'Reilly, S.; Boufford, J. I.; Breysse, P. N.; Chiles, T.; Mahidol, C.; Coll-Seck, A. M.; Cropper, M. L.; Fobil, J.; Fuster, V.; Greenstone,

480 M.; Haines, A.; Hanrahan, D.; Hunter, D.; Khare, M.; Krupnick, A.; Lanphear, B.; Lohani, B.; Martin, K.; Mathiasen, K. V.; McTeer, M. A.; Murray, C. J. L.; Ndahimananjara, J. D.; Perera, F.; Potočnik, J.; Preker, A. S.; Ramesh, J.; Rockström, J.; Salinas, C.; Samson, L. D.; Sandilya, K.; Sly, P. D.; Smith, K. R.; Steiner, A.; Stewart, R. B.; Suk, W. A.; van Schayck, O. C. P.; Yadama, G. N.; Yumkella, K.; Zhong, M. The Lancet Commission on Pollution and Health. *The Lancet*. 2018. https://doi.org/10.1016/S0140-6736(17)32345-0.

485 Lu, T.; Liu, Y.; Garcia, A.; Wang, M.; Li, Y.; Bravo-villasenor, G.; Campos, K.; Xu, J.; Han, B. Leveraging Citizen Science and Low-Cost Sensors to Characterize Air Pollution Exposure of Disadvantaged Communities in Southern California. *Int J Environ Res Public Health* **2022**, *19* (14). https://doi.org/10.3390/ijerph19148777.

Lunden, M. M.; Parworth, C. L.; Barkjohn, K. K.; Holder, A. L.; Frederick, S. G.; Clements, A. L. Correction and Accuracy of PurpleAir PM 2.5 Measurements for Extreme Wildfire Smoke. **2022**. https://doi.org/10.3390/s22249669.

490 Magi, B. I.; Cupini, C.; Francis, J.; Green, M.; Hauser, C. Evaluation of PM2.5 Measured in an Urban Setting Using a Low-Cost Optical Particle Counter and a Federal Equivalent Method Beta Attenuation Monitor. *Aerosol Science and Technology* **2020**, *54* (2). https://doi.org/10.1080/02786826.2019.1619915.

Malings, C.; Tanzer, R.; Hauryliuk, A.; Saha, P. K.; Robinson, A. L.; Presto, A. A.; Subramanian, R. Fine Particle Mass Monitoring with Low-Cost Sensors: Corrections and Long-Term Performance Evaluation. *Aerosol Science and Technology* **2020**, *54* (2). https://doi.org/10.1080/02786826.2019.1623863.

Maugis, C.; Celeux, G.; Martin-Magniette, M. L. Variable Selection for Clustering with Gaussian Mixture Models. *Biometrics* **2009**, *65* (3). https://doi.org/10.1111/j.1541-0420.2008.01160.x.

McFarlane, C.; Raheja, G.; Malings, C.; Appoh, E. K. E.; Hughes, A. F.; Westervelt, D. M. Application of Gaussian Mixture Regression for the Correction of Low Cost PM2.5Monitoring Data in Accra, Ghana. *ACS Earth Space Chem* **2021**, *5* (9). https://doi.org/10.1021/acsearthspacechem.1c00217.

Olstrup, H.; Johansson, C.; Forsberg, B.; Tornevi, A.; Ekebom, A.; Meister, K. A Multi-Pollutant Air Quality Health Index (AQHI) Based on Short-Term Respiratory Effects in Stockholm, Sweden. *Int J Environ Res Public Health* **2019**, *16* (1). https://doi.org/10.3390/ijerph16010105.

Pope, C. A.; Dockery, D. W. Health Effects of Fine Particulate Air Pollution: Lines That Connect. *J Air Waste Manage Assoc* **2006**, *56* (6). https://doi.org/10.1080/10473289.2006.10464485.

Raftery, A. E.; Dean, N. Variable Selection for Model-Based Clustering. *J Am Stat Assoc* **2006**, *101* (473). https://doi.org/10.1198/016214506000000113.

Raheja, G.; Nimo, J.; Appoh, E. K. E.; Essien, B.; Sunu, M.; Nyante, J.; Amegah, M.; Quansah, R.; Arku, R. E.; Penn, S. L.; Giordano, M. R.; Zheng, Z.; Jack, D.; Chillrud, S.; Amegah, K.; Subramanian, R.; Pinder, R.; Appah-Sampong, E.; Tetteh, E. N.; Borketey, M. A.; Hughes, A. F.; Westervelt, D. M. Low-Cost Sensor Performance Intercomparison, Correction Factor Development, and 2+ Years of Ambient PM2.5 Monitoring in Accra, Ghana. *Environ Sci Technol* **2023**, *57* (29). https://doi.org/10.1021/acs.est.2c09264.

Rueda, E. M.; Carter, E.; Orange, C. L. '; Quinn, C.; Volckens, J. Size-Resolved Field Performance of Low-Cost Sensors for Particulate Matter Air Pollution. *Cite This: Environ. Sci. Technol. Lett* **2023**, *10*, 247–253. https://doi.org/10.1021/acs.estlett.3c00030.

Sayahi, T.; Butterfield, A.; Kelly, K. E. Long-Term Field Evaluation of the Plantower PMS Low-Cost Particulate Matter Sensors. *Environmental Pollution* **2019**, *245*. https://doi.org/10.1016/j.envpol.2018.11.065.

Shi, J. Q.; Choi, T. *Gaussian Process Regression Analysis for Functional Data*; 2011. https://doi.org/10.1201/b11038.

Snyder, E. G.; Watkins, T. H.; Solomon, P. A.; Thoma, E. D.; Williams, R. W.; Hagler, G. S. W.; Shelow, D.; Hindin, D. A.; Kilaru, V. J.; Preuss, P. W. The Changing Paradigm of Air Pollution Monitoring. *Environ Sci Technol* **2013**, *47* (20). https://doi.org/10.1021/es4022602.

Stavroulas, I.; Grivas, G.; Michalopoulos, P.; Liakakou, E.; Bougiatioti, A.; Kalkavouras, P.; Fameli, K. M.; Hatzianastassiou, N.; Mihalopoulos, N.; Gerasopoulos, E. Field Evaluation of Low-Cost PM Sensors (Purple Air PA-II) Under Variable Urban Air Quality Conditions, in Greece. *Atmosphere (Basel)* **2020**, *11* (9). https://doi.org/10.3390/atmos11090926.

525 Tryner, J.; L'Orange, C.; Mehaffy, J.; Miller-Lionberg, D.; Hofstetter, J. C.; Wilson, A.; Volckens, J. Laboratory Evaluation of Low-Cost PurpleAir PM Monitors and in-Field Correction Using Co-Located Portable Filter Samplers. *Atmos Environ* **2020**, *220*. https://doi.org/10.1016/j.atmosenv.2019.117067.

U.S. Environmental Protection Agency (EPA). *Air Quality System (AQS)*. https://www.epa.gov/aqs.

U.S. Environmental Protection Agency. *AirNow API*. www.docs.airnowapi.org/Data/query.

530 U.S. Environmental Protection Agency. *List of Designated Reference and Equivalent Methods*; Research Triangle Park, NC 27711, 2023.

Wallace, L.; Bi, J.; Ott, W. R.; Sarnat, J.; Liu, Y. Calibration of Low-Cost PurpleAir Outdoor Monitors Using an Improved Method of Calculating PM2.5. *Atmos Environ* **2021**, *256*. https://doi.org/10.1016/j.atmosenv.2021.118432.

Yuan, C.; Yang, H. Research on K-Value Selection Method of K-Means Clustering Algorithm. *J (Basel)* **2019**, *2* (2). 535 https://doi.org/10.3390/j2020016.

Zheng, T.; Bergin, M. H.; Johnson, K. K.; Tripathi, S. N.; Shirodkar, S.; Landis, M. S.; Sutaria, R.; Carlson, D. E. Field Evaluation of Low-Cost Particulate Matter Sensors in High-and Low-Concentration Environments. *Atmos Meas Tech* **2018**, *11* (8), 4823–4846. https://doi.org/10.5194/amt-11-4823-2018.

Zusman, M.; Schumacher, C. S.; Gassett, A. J.; Spalt, E. W.; Austin, E.; Larson, T. V.; Carvlin, G.; Seto, E.; Kaufman, J. D.; 540 Sheppard, L. Calibration of Low-Cost Particulate Matter Sensors: Model Development for a Multi-City Epidemiological Study. *Environ Int* **2020**, *134*. https://doi.org/10.1016/j.envint.2019.105329.